Performance Optimization of the Reflector Antenna for the Digital Beam-Forming SAR System

A. Patyuchenko, M. Younis, S. Huber, and G. Krieger
Microwaves and Radar Institute, German Aerospace Center (DLR)
Muenchener Str. 20, 82234 ***Wessling, Germany***
Phone: +49(0)8153 28 3381, Fax: +49(0)8153 28 1449
anton.patyuchenko@dlr.de

INTRODUCTION

A novel idea of a realization a Synthetic Aperture Radar (SAR) system combining a reflector antenna with a digital feed array was suggested for the first time in [1]. The new digital beam-forming (DBF) SAR architecture has better overall system performance while being of lower complexity level as compared to the planar antenna based architecture [2]. This innovative idea has driven intensive studies aimed at future space borne SAR missions.

Antenna design aspects and performance of the reflector based DBF SAR system have been thoroughly discussed in [2], [3] and [4]. As shown in [3] the initial design of the reflector antenna, aimed to satisfy the main system requirements, may need further optimization to allow better system performance. This paper is dedicated to this problem.

The paper starts with the introduction of the initial system design and its operational principle. The discussion is followed by the consideration of several aspects specific for the reflector based DBF SAR and their impact on the system performance. Possible ways to reduce the impact by optimizing the antenna design are suggested. In the end the overall system performance is estimated.

INITIAL DESIGN OF THE REFLECTOR BASED DBF SAR SYSTEM

A simplified structure of the initial design of the digital beam-forming SAR system based on the reflector antenna is depicted in Fig. 1. It consists of a circular paraboloid, a linear array of feed antennas, a feed system circuitry and a digital control system. The feed array is represented by sub-arrays linearly arranged with a separation d and placed in the reflector's focal plane. Each feed element is connected to a TR module. The receive part is represented by a switch, a low noise amplifier, a band-pass filter, and an analog-to-digital converter. In the transmit part a conventional analog configuration based on phase shifters is used.

Activation of a single element results in a narrow high-gain beam illuminating a certain portion of the swath. Combination of several channels results in formation of the required antenna pattern. When all the elements are switched on, the reflector antenna pattern covers the complete swath by a wide low-gain beam. The initial system design uses a single digital channel in azimuth and is operated in Scan-On-Receive (SCORE) mode [5], [6]: the ground swath of interest is illuminated by the wide transmit beam and a narrow receive beam scans over the entire swath following the pulse on ground. The scanning is performed digitally by combining weighted data from the activated signal channels

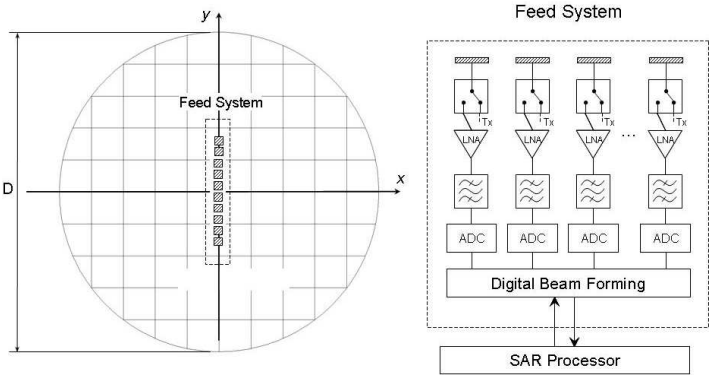

Fig. 1. Simplified architecture of the reflector based DBF SAR system: the reflector dish with a schematically depicted feed system (left) and a simplified structure of the digital feed system circuitry (right).

according to:

$$s_{out}(t) = \sum_{i=1}^{N} w_i(t) \cdot s_{in_i}(t), \tag{1}$$

where N is the total number of elements, $w_i(t)$ are complex weighting coefficients, $s_{in_i}(t)$ is the input signal at the i^{th} channel, $s_{out}(t)$ is the output signal.

The parameters of the initial reflector antenna design and the DBF SAR system specifications are described in Table I a) and b) correspondingly [3]. The antenna is represented by the circular parabolic dish of $10\,\mathrm{m}$ diameter with 34 primary feed elements located at a distance of $5.5\,\mathrm{m}$ from the center of the reflector. The system is operated at C-Band at an orbit height of $710\,\mathrm{km}$ with a repeat cycle of around 14 days.

TABLE I

(a) Antenna Parameters

Parameter	Value
operational frequency	$5.3\,\mathrm{GHz}$
diameter	$10\,\mathrm{m}$
focal length	$5.5\,\mathrm{m}$
number of elements	34
inter-element spacing	$0.6 \cdot \lambda$
feed array length	$1.14\,\mathrm{m}$

(b) System Specifications

Parameter	Value
average transmitted power	$68\,\mathrm{W}$
duty cycle	$\eta = 5\%$
bandwidth	$100\,\mathrm{MHz}$
ground swath width	$203\,\mathrm{km}$
repeat cycle	14 days
look angles	$30^\circ - 40^\circ$
orbit height	$710\,\mathrm{km}$

SYSTEM PERFORMANCE ASPECTS: ANALYSIS AND OPTIMIZATION

Frequency Dependence of the Antenna Patterns

In this section we investigate the impact of the frequency dependent radiation characteristics of the reflector antenna on the DBF SAR system performance.

As shown in Fig. 2 a), a far field radiation pattern of the reflector antenna, C_{total}, can be represented as a sum of its three main components, (2): C_1 - a far field pattern due to the currents induced on the reflector dish by a primary field, C_2 - a far field pattern due to the currents induced on the feed system by the field reflected from the dish, C_3 - a far field pattern due to the currents induced on the reflector by the field reflected from the feed system. The total field is expressed as:

$$C_{total}(\theta, \phi, f) = C_1(\theta, \phi, f) + C_2(\theta, \phi, f) + C_3(\theta, \phi, f) + C_i \tag{2}$$

where θ is the elevation angle, ϕ is the azimuth angle, f is the frequency, and C_i are higher order components (neglected in the current analysis).

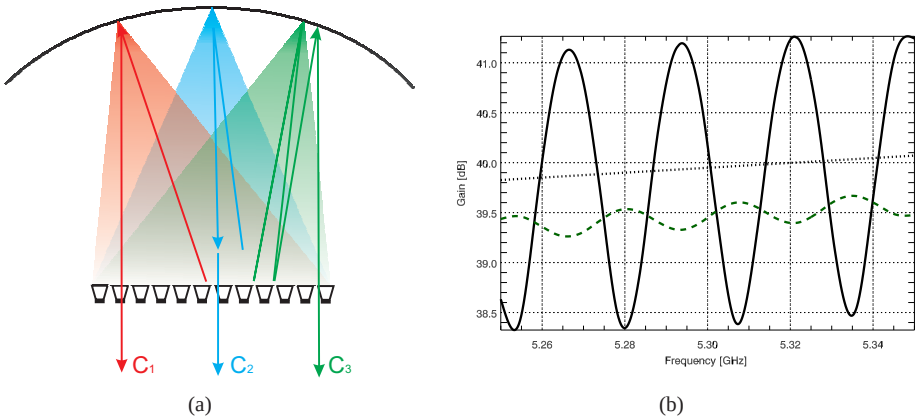

(a) (b)

Fig. 2. a) Far field radiation pattern components. b) Tx gain at zero scan angle as a function of frequency: solid line - initial design (total gain), dotted line - initial design (first component), dashed line - initial design with 0.8 m feed offset in Y direction (total gain).

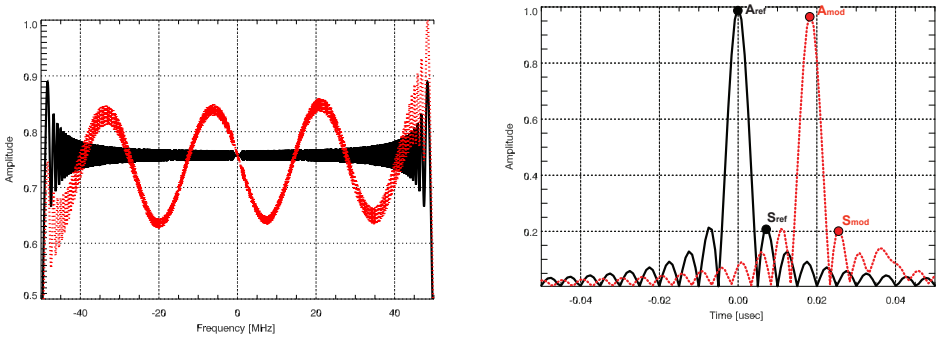

(a) (b)

Fig. 3. a) Reference and modulated receive signals at the input of the range compression filter in frequency domain b) Reference and modulated receive signals at the output of the range compression filter in time domain (solid line - reference signal, dotted line - modulated signal).

In Fig. 2 b) the gain variation of the total far field transmit pattern, $C_{total,Tx}$, at zero scan angle for the initial symmetric reflector configuration (solid line) is compared with a design using a feed offset of $0.8\,\mathrm{m}$ in Y direction (dashed line). The gain variation of the first field component, $C_{1,Tx}$, for the initial design (no blockage present) is represented by the dotted line. The obtained results demonstrate that the blockage due to the feed system located in the main beam has a strong impact on the frequency dependence of the antenna characteristics. This effect can be mitigated by using an offset configuration. In the following we evaluate the impact of the frequency variation effect on the reflector based DBF SAR system for the initial and offset designs.

A magnitude spectrum of the chirp echo signal received by the considered DBF SAR from the swath center, $\theta = 0°, \phi = 0°$, is depicted in Fig. 3 a). Here the dotted line represents a modulated signal, $S_{mod}(f_r)$, given by the ideal chirp of which each frequency component is weighted with the complex two way antenna field pattern value obtained for the corresponding frequencies at the given scan angle; the solid line represents a non-modulated reference signal, $S_{ref}(f_r)$. The signals are described by the following equations:

$$S_{ref}(f_r) = \mathcal{F}\{\exp(j\pi k_r t^2) \cdot rect\left(\frac{t}{T_p}\right)\} \cdot C_{total,Tx,Rx}(0°, 0°, f_0)$$
$$S_{mod}(f_r) = \mathcal{F}\{\exp(j\pi k_r t^2) \cdot rect\left(\frac{t}{T_p}\right)\} \cdot C_{total,Tx,Rx}(0°, 0°, f)$$

where t is the time, T_p is the pulse duration, k_r is the range modulation rate, f_0 is the radar center frequency and f are frequencies of the operational band.

After the chirps pass a range compression filter the impulse response takes a form depicted in Fig. 3 b). Values $A_{ref,mod}$ and $S_{ref,mod}$, depicted on the plot, represent an amplitude and a side lobe level of the compressed signals correspondingly. The impulse response analysis of the DBF SAR system was performed for each scan angle of interest using the following evaluation parameters: Peak Ratio defined as A_{mod}/A_{ref}, Relative Peak-to-Side Lobe

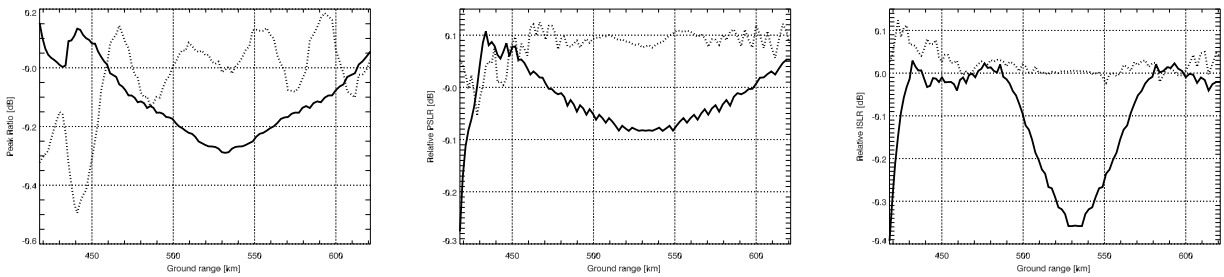

(a) (b) (c)

Fig. 4. a) Peak Ratio, b) Relative Peak-to-Side Lobe Ratio and c) Relative Integrated Side Lobe Ratio as a function of the ground range. Solid line - initial symmetric configuration, dotted line - offset configuration with an offset height of 0.8 m in Y direction.

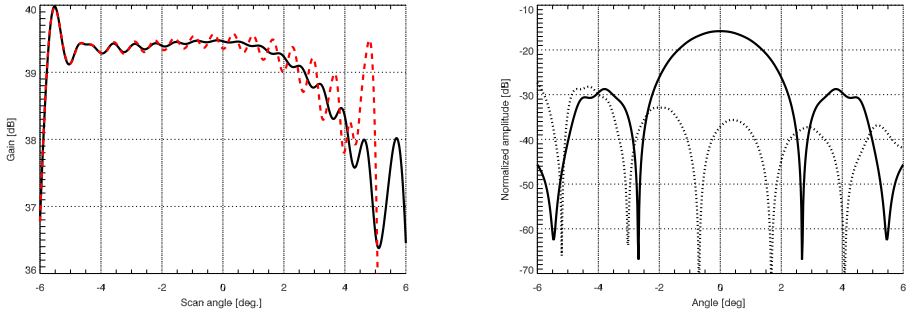

(a) (b)

Fig. 5. a) Transmit antenna patterns without (solid line) and with (dashed line) phase correction (0.8 m offset design, blockage is neglected). b) The level of the "ghost" Tx signal relative to the useful signal as a function of the scan angle (solid line - initial symmetric design, dotted line - 0.8 m offset design).

Ratio (PSLR) expressed as $(S_{ref} \cdot P_{mod})/(P_{ref} \cdot S_{mod})$ and Relative Integrated Side Lobe Ratio (ISLR) found as $ISLR_{ref}/ISLR_{mod}$ where $ISLR$ is the sum of energy in the side lobes divided by the sum of energy in the main lobe.

In Fig. 4 the results of the system impulse response analysis obtained for the initial symmetric configuration (solid line) are compared with the $0.8\,\mathrm{m}$ offset design (dotted line). The degradation of the Peak Ratio for the offset configuration at near ranges is due to the filter mismatch. In general, the analysis shows that the offset configuration with a less pronounced frequency variation effect allows to achieve better overall performance in terms of the power content of the impulse response as well as of the side lobe level compared to the reference signal.

Transmit Antenna Pattern Shape Improvement

The offset configuration leads to the degradation of the antenna pattern. The shape of the transmit elevation pattern has an impact on the system ambiguities level as well as on the radiometric resolution. Activation of all the feed elements according to equation (1), with $w_i(t) = 1$, results in the transmit pattern depicted by the solid line in Fig. 5 a). The pattern has a large gain loss at large scan angles which leads to a performance degradation at the swath borders. The shape of the pattern can be improved by means of pattern synthesis methods. In Fig. 5 a) the dashed line represents the pattern formed when complex weights are applied to the first three digital channels. The pattern synthesis required the smallest variation of the electric field over the angular range of interest. In order to further decrease the gain loss at large scan angles the number of feed elements was increased from 34 to 38.

Multipath Effect

The large feed system structure in the near field results in the formation of a so called ghost chirp due to multipath effects. This disturbing signal is a result of the third component, C_3, of the antenna radiation pattern, C_{total} Fig. 2 a). The "ghost" signal is following the useful signal on ground and in the end effect this may cause an image quality degradation. In Fig. 5 b) a level of the disturbing transmit signal relative to a useful signal is shown as a function of scan angle for the initial (solid line) and offset (dotted line) reflector configurations. A level of the disturbing signal on receive is well below -35 dB for the given direction using both configurations. The results demonstrate that the feed offset tends to push the maximum of the disturbing pattern component out of the angular range of interest.

PERFORMANCE OF THE REFLECTOR BASED DBF SAR SYSTEM

In Fig. 6 the performance of the DBF SAR system based on the initial reflector design is compared to the system using the reflector antenna with a 0.8 m offset height and phase correction. The level of Azimuth-Ambiguity-to-Signal Ratio ($AASR$) is higher at the swath borders for the optimized system. This is explained by the increased defocusing for the large scan angles which in turn leads to broader azimuth patterns. In order to reduce this effect a transmit pulse repetition frequency was increased from 1830 MHz up to 1995 MHz, which allowed to improve the azimuth ambiguities level over the complete swath as well. The Range-Ambiguity-to-Signal Ratio ($RASR$) and Noise-Equivalent-Sigma-

Zero ($NESZ$) levels remain generally unchanged and are well below typical requirements. Nevertheless at near ranges these parameters are worse which is due to the increased pulse repetition frequency and the reduced transmit gain for the offset design. The azimuth resolution of $8\,\mathrm{m}$ remained unchanged for both systems.

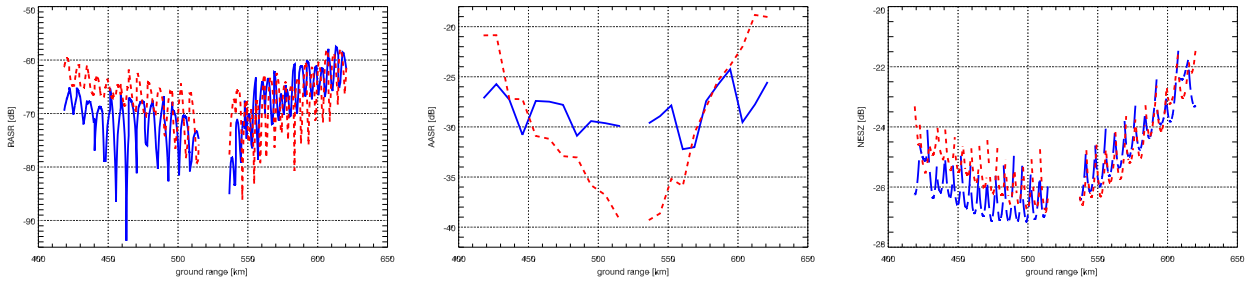

(a) (b) (c)

Fig. 6. a) Range Ambiguity-to-Signal Ratio b) Azimuth Ambiguity-to-Signal Ratio c) Noise-Equivalent-Sigma-Zero (solid line - initial symmetric design, dashed line - 0.8 m offset design with the Tx pattern phase correction).

CONCLUSION

Performance aspects, specific for the novel DBF SAR system in combination with a reflector antenna, are considered in this paper. The main discussion is dedicated to the problem of frequency dependent antenna patterns and the impact of this effect on the DBF SAR system performance. It was shown that the blockage due to the feed system located in the antenna main beam has a strong influence on the frequency variation effect. An offset reflector configuration was considered as a possible solution to the problem. After pattern optimization, the performance of the DBF SAR based on the offset design was estimated and compared to the initial symmetric system. It was shown that the optimized system has a low ambiguity level and a radiometric resolution comparable to the reference design, while it has less impact on the signal frequency modulation and is characterized by the reduced level of multipath effects.

Optimization of a complex system for a single parameter usually leads to the degradation of another system characteristic, although a certain compromise to improve the required parameter keeping the overall performance on a high level can be found. This was in particular demonstrated in this paper which showed that the DBF SAR system based on the reflector antenna is a promising concept requiring further development and intensive investigations.

REFERENCES

[1] G. Krieger, N. Gebert, M. Younis, F. Bordoni, A. Patyuchenko, and A. Moreira, “Advanced concepts for ultra-wide swath SAR imaging,” in *Proc. 7th European Conference on Synthetic Aperture Radar (EUSAR’08)*, Friedrichshafen, Germany, June 2008.

[2] M. Younis, S. Huber, A. Patyuchenko, F. Bordoni, and G. Krieger, “Performance comparison of reflector- and planar-antenna based digital beam-forming SAR,” *International Journal of Antennas and Propagation (Special Issue on Active Antennas for Space Applications)*, 2009. [Online]. Available: http://www.hindawi.com/journals/ijap/2009/614931.html

[3] A. Patyuchenko, M. Younis, S. Huber, F. Bordoni, and G. Krieger, “Design aspects and performance estimation of the reflector based digital beam-forming SAR system,” in *Proc. International Radar Symposium (IRS’09)*, Hamburg, Germany, Sept. 2009.

[4] M. Younis, S. Huber, A. Patyuchenko, F. Bordoni, and G. Krieger, “Digital beam-forming for spaceborne reflector- and planar-antenna SAR a system performance comparison ,” in *Proc. IEEE International Geoscience and Remote Sensing Symposium (IGARSS’09)*, Cape Town, South Africa, July 2009.

[5] M. Suess and W. Wiesbeck, “Side looking SAR system,” Patent 20 040 150 547, Mar. 30, 2004.

[6] B. G. M. Suess and R. Zahn, “A novel high resolution, wide swath SAR,” in *Proc. IEEE International Geoscience and Remote Sensing Symposium (IGARSS’01)*, vol. 3, 2003, pp. 1013–1015.